Anal. Chem. **1998,** *70,* 780−791

Intelligent Polymerized Crystalline Colloidal Arrays: Novel Chemical Sensor Materials

John H. Holtz, Janet S. W. Holtz, Calum H. Munro, and Sanford A. Asher*

Department of Chemistry and Materials Research Center, University of Pittsburgh, Pittsburgh, Pennsylvania 15260

We report the development of a novel sensing material that reports on analyte concentrations via diffraction of visible light from a polymerized crystalline colloidal array (PCCA). The PCCA is a mesoscopically periodic crystalline colloidal array (CCA) of spherical polystyrene colloids polymerized within a thin, intelligent polymer hydrogel film. CCAs are brightly colored, and they efficiently diffract visible light meeting the Bragg condition. The intelligent hydrogel incorporates chemical molecular recognition agents that cause the gel to swell in response to the concentration of particular analytes; the gel volume is a function of the analyte concentration. The color diffracted from the hydrogel film is, thus, a function of analyte concentration: the swelling of the gel changes the periodicity of the CCA, which results in a shift in the diffracted wavelength. We have fabricated a sensor, utilizing a crown ether as the recognition agent, that detects Pb^{2+} in the 0.1 μM−20mM (∼20 ppb−∼4000 ppm) concenration range. We have also fabricated glucose and galactose sensors, utilizing glucose oxidase or β-D-galactosidase as the recognition elements. The glucose oxidase sensor detects glucose in the 0.1−0.5 mM (18−90 ppm) concentration range in the presence of oxygen and detects as little as 10^{-12} M glucose (0.18 ppt) in the absence of oxygen. In addition, this sensor reports on dissolved oxygen concentration from ∼1 to 6 ppm in the presence of constant glucose concentrations.

We have developed a novel sensing material that reports on analyte concentrations via diffraction of visible light from a polymerized crystalline colloidal array (PCCA).[1−3] The PCCA is a mesoscopically periodic crystalline colloidal array (CCA) of spherical polystyrene colloids polymerized within a thin, intelligent polymer hydrogel film. CCAs are brightly colored; they efficiently diffract visible light meeting the Bragg condition. The intelligent hydrogel incorporates chemical molecular recognition agents that cause the gel to swell in response to the concentration of particular analytes;[4−16] the gel volume is a function of the analyte concentration. The color diffracted from the hydrogel film is, thus, a function of analyte concentration: the swelling of the gel changes the periodicity of the CCA,[1−3] which results in a shift in the diffracted wavelength. We have fabricated a sensor, utilizing a crown ether as the recognition agent, that detects Pb^{2+} in the 0.1 μM−20 mM (∼20 ppb−∼4000 ppm) concentration range. We have also fabricated glucose and galactose sensors, utilizing glucose oxidase or β-D-galactosidase as the recognition elements. The glucose oxidase sensor detects glucose in the 0.1−0.5 mM (18−90 ppm) concentration range in the presence of oxygen and detects as little as 10^{-12} M glucose (0.18 ppt) in the absence of oxygen. In addition, this sensor reports on dissolved oxygen concentrations from ∼1 to 6 ppm in the presence of constant glucose concentrations.

CCAs self-assemble from suspensions of highly charged, monodisperse colloidal particles (Figure 1).[3a,17−27] At low ionic

* Corresponding author. Phone: 412-624-8570. Fax: 412-624-0588. E-mail: asher+@pitt.edu.

(1) (a) Holtz, J. H; Asher, S. A. *Nature* **1997**, *389*, 829. (b) Asher, S. A.; Holtz, J.; Liu, L.; Wu, Z. *J. Am. Chem. Soc.* **1994**, *116*, 4997.
(2) Weissman, J. M.; Sunkara, H. B.; Tse, A. S.; Asher, S. A. *Science* **1996**, *274*, 959.
(3) (a) Asher, S. A.; Weissman, J. M.; Sunkara, H. B.; Pan, G.; Holtz, J.; Liu, L.; Kesavamoorthy, R. In *Polymers for Advanced Optical Applications*; Jenekhe, S. A., Wynne, K. J., Eds.; Washington, DC, 1997. (b) Asher, S. A. U.S. Patents 4,627,689 and 4,632,517, 1986. (c) Haacke, G.; Panzer H. P.; Magliocco, L. G.; Asher, S. A. U.S. Patent 5,266,238, 1993. (d) Asher, S. A.; Chang, S. Y.; Jagannathan, S.; Kesavamoorthy, R.; Pan, G. U.S. Patent 5,452,123, 1995. (e) Asher, S. A.; Jagannathan, S. U.S. Patent 5,281,370, 1994. (f) Pan, G. In *Nanoparticles in Solids and Solutions*; Fendler, J. H., Dekany, I., Eds.; NATO ASI Series 18; Kluwer Academic Publishers: Dordrecht, 1996; pp 65−69.
(4) Irie, M. *Adv. Polym. Sci.* **1993**, *110*, 49.
(5) Osada, Y.; Gong, J. *Prog. Polym. Sci.* **1993**, *18*, 187.
(6) Galayev, I. *Russ. Chem. Rev.* **1995**, *64*, 471.
(7) Gerkhe, S. H. *Adv. Polym. Sci.* **1993**, *110*, 81.
(8) Kishi, R.; Hara, M.; Sawahata, K.; Osada, Y. In *Polymer Gels*; DeRossi, et al., Eds.; Plenum: New York, 1991.
(9) Osada, Y. *Adv. Polm. Sci.* **1987**, *82*, 1.
(10) Irie, M.; Misumi, Y.; Tanaka, T. *Polymer* **1993**, *34*, 4531.
(11) Kikuchi, A.; Suzuki, K.; Okabayashi, O.; Hoshino, H.; Kataoka, K.; Sakurai, Y.; Okano, T. *Anal. Chem.* **1996**, *68*, 823.
(12) McCurley, M. F. *Biosens. Bioelectron.* **1994**, *9*, 527.
(13) McCurley, M. F.; Seitz, W. R. *Anal. Chim. Acta* **1991**, *249*, 373.
(14) Sheppard, N. F.; Lesho, M. J.; McNally, P.; Francomacaro A. S. *Sens. Actuators B* **1995**, *28*, 95.
(15) Schalkhammer, T.; Lobmaier, C.; Pittner, F.; Leitner, A.; Brunner, H.; Aussenegg F. R. *Sens. and Actuators B* **1995**, *24/25*, 166.
(16) Schalkhammer, T.; Lobmaier, C.; Pittner, F.; Leitner, A.; Brunner, H.; Aussenegg F. R. *Mikrochim. Acta* **1995**, *121*, 259.
(17) Brnardic, C. M.S. Thesis, University of Pittsburgh, 1990.
(18) Krieger, I. M.; O'Neil, F. M. *J. Am. Chem. Soc.* **1968**, *90*, 3114.
(19) Hiltner, P. A.; Krieger, I. M. *J. Phys. Chem.* **1969**, *73*, 2386.
(20) Hiltner, P. A.; Papir, Y. S.; Krieger, I. M. *J. Phys. Chem.* **1971**, *75*, 1881.
(21) Clark, N. A.; Hurd, A. J.; Ackerson, B. J. *Nature* **1979**, *281*, 57.
(22) Ackerson, B. J.; Clark, N. A. *Phys. Rev. Lett.* **1981**, *46*, 123.
(23) Aastuen, D. J. W.; Clark, N. A.; Cotter L. K.; Ackerson, B. J. *Phys. Rev. Lett.* **1986**, *57*, 1733.
(24) Hurd, A. J.; Clark, N. A.; Mockler, R. C.; O'Sullivan, W. *Phys. Rev. A.* **1982**, *26*, 2869.
(25) Asher, S. A.; Flaugh, P. L.; Washinger, G. *Spectroscopy* **1986**, *1*, 26.

S0003-2700(97)00853-6 CCC: $15.00
Published on Web 01/21/1998

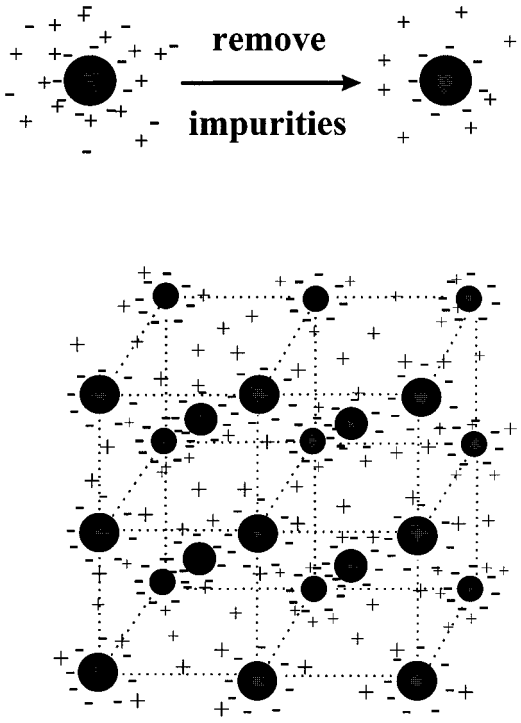

Figure 1. Self-assembly of a body-centered cubic CCA. At low ionic strengths, repulsion between monodisperse, highly charged colloidal particles forces the colloidal spheres into a minimum energy configuration, which is either a body- or face-centered cubic lattice.

strengths, the colloidal particles repel each other, and the system assumes a minimum energy configuration, which is usually a body- or face-centered cubic lattice. The colloidal particles may be composed of inorganic materials such as silica or organic polymers such as poly(methyl methacrylate), polystyrene, or poly(*N*-isopropylacrylamide).[2,17−29]

The periodicity of the CCA is on the order of ~200 nm, so the CCA diffracts visible light. The diffraction is in the "dynamical diffraction regime" and almost obeys Bragg's law:[27,30]

$$m\lambda = 2nd \sin \theta$$

where m is the order of diffraction, λ is the diffracted wavelength in vacuum, n is the refractive index of the system (solvent, hydrogel, and colloids), d is the spacing between the diffracting planes (for the CCAs presented here, the 110 planes of a BCC lattice), and θ is the glancing angle between the incident light propagation direction and the diffracting planes.

We have developed methods to polymerize the CCA in a hydrogel film to form a PCCA.[1−3] We dissolve nonionic polymerizable monomers, cross-linkers, and photoinitiators into the liquid CCA. The monomer is usually acrylamide or an acrylamide derivative. We then photopolymerize the mixture in a quartz cell to make a thin, diffracting PCCA film. The PCCA films have applications as tunable filters, optical switches, and nonlinear optical devices.[2,3,25,31]

To make a sensor, we polymerize a chemically sensitive, intelligent hydrogel around a liquid CCA, resulting in an intelligent PCCA (IPCCA). Intelligent hydrogels are water swollen, cross-linked networks of polymers that reversibly change volume in response to specific stimuli.[4−16] The constituent polymers of chemically sensitive intelligent gels incorporate molecular recognition elements. When these molecular recognition elements interact with specific substrates, the monomer units bearing the recognition elements undergo either a change in solubility or a change in charge state. Changes in solubility will cause the polymer chains of the network to swell or contract. Changes in the charge state result in changes in the interactions between these charged groups and alterations in the concentration of electrolytes inside the gel. Either effect results in changes in the hydrogel volume.

This gel volume response makes intelligent hydrogels potentially useful for chemomechanical systems,[4−10] separations devices,[38−40] and sensors.[11−16] The method of detection may be electrochemical,[11,14] mechanical,[34] or optical.[12,13,15,16] Published methods for optical detection of the volume response include fluorescence,[12] reflection into a waveguide,[13] or interferometry.[15,16]

Our sensor utilizes a CCA immobilized within a chemically sensitive intelligent hydrogel to optically report on small changes in the hydrogel volume (Figure 2). As the volume of the intelligent hydrogel isotropically changes due to the interactions of the molecular recognition agent with its substrate, the lattice spacing of the CCA changes, causing the diffracted wavelength to shift in accordance with Bragg's law. The IPCCA is well suited for sensor applications due to the ease with which we can directly measure volume changes of the hydrogel by monitoring the CCA-diffracted wavelength.

EXPERIMENTAL SECTION

Sensor Fabrication. Highly charged, monodisperse polystyrene colloids were prepared by emulsion polymerization, as described elsewhere.[17] The CCAs used in this study were 5−7 wt % suspensions of ~110 nm polystyrene colloidal particles. Excess ions and surfactants were removed from the colloidal suspension by dialysis against deionized water. The dialyzed suspension was further cleaned by shaking with ion-exchange resin (Bio-Rad). After being shaken with ion-exchange resin, the suspension became iridescent due to Bragg diffraction from the CCA.

(26) Rundquist, P. A.; Jagannathan, S.; Kesavamoorthy, R.; Brnardic, C.; Xu, S.; Asher, S. A. *J. Chem. Phys.* **1990**, *94*, 711.
(27) Carlson, R. J.; Asher, S. A. *Appl. Spectrosc.* **1984,** *38*, 297.
(28) Chang, S.-Y.; Liu, L.; Asher, S. A. *J. Am. Chem. Soc.* **1994,** *116*, 6739.
(29) Chang, S.-Y.; Liu, L.; Asher, S. A. *J. Am. Chem. Soc.* **1994**, *116*, 6745.
(30) (a) Rundquist, P. A.; Kesavamoorthy, R.; Jagannathan, S.; Asher, S. A. *J. Chem. Phys.* **1991**, *95*, 1249. (b) Rundquist, P. A.; Photinos, P.; Jagannathan, S.; Asher, S. A. *J. Chem. Phys.* **1989**, *91*, 4932.
(31) Pan, G.; Kesavamoorthy, R.; Asher, S. A. *Phys. Rev. Lett.* **1997**, *78*, 3860.
(32) Asher, S. A.; Bormett, R. W.; Chen, X. G.; Lemmon, D. H.; Cho, N.; Peterson, P.; Arrigoni, M.; Spinelli, L.; Cannon, J. *Appl. Spectrosc.* **1993**, *47*, 628.
(33) Li, Y.; Tanaka, T. *Annu. Rev. Mater. Sci.* **1992**, *22*, 243.
(34) Tanaka, T.; Fillmore, D.; Sun, S. T.; Nishio, I.; Swislow, G.; Shah, A. *Phys. Rev. Lett.* **1980**, *45*, 1636.
(35) Hirotsu, S.; Hirokawa, Y.; Tanaka, T. *J. Chem. Phys.* **1987**, *87*, 1392.
(36) Flory, P. J. *Principles of Polymer Science*; Cornell University Press: Ithaca, NY, 1953.
(37) Kurnikova, M.; Holtz, J. H.; Coalson, R. D.; Asher, S. A. Unpublished results.
(38) Wang, K. L.; Burban, J. H.; Cussler E. L. *Adv. Polym. Sci.* **1993**, *110*, 67.
(39) Gehrke, S. H.; Andrews, G. P.; Cussler, E. L. *Chem. Eng. Sci.* **1986**, *41*, 2153.
(40) Grimshaw, P. E.; Grodzinski, A. J.; Yarmush, M. L.; Yarmush, D. M. *Chem. Eng. Sci.* **1989**, *44*, 827.

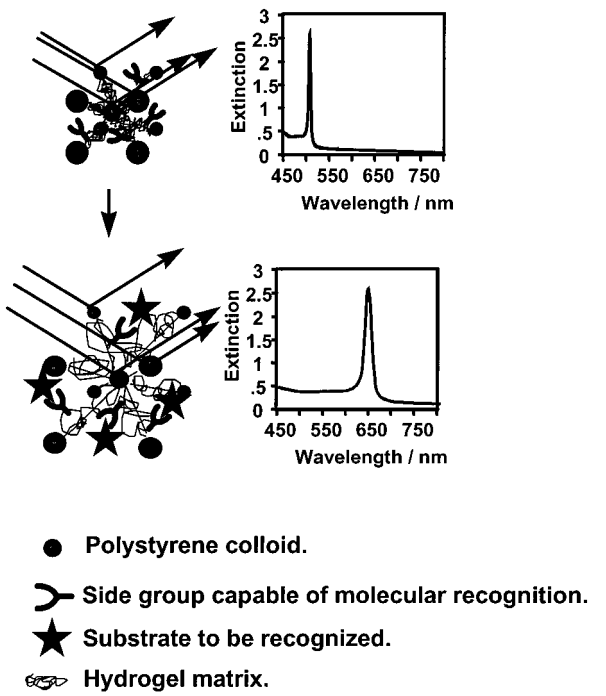

Figure 2. General motif for the intelligent polymerized crystalline colloidal array (IPCCA) sensors. The CCA Bragg diffraction is a sensitive monitor of the hydrogel volume change induced by the interaction or binding of the molecular recognition agent to a substrate. In principle, any molecular recognition agent can be attached to the hydrogel polymer to produce an IPCCA sensor.

In order to fabricate a PCCA, monomers such as acrylamide (AMD) (Acros Organics) or *N*-isopropylacrylamide (NIPA) (Acros Organics), cross-linkers such as *N*,*N*′-methylenebisacrylamide (bis-AMD) (Acros Organics), and a UV photoinitiator such as diethoxyacetophenone (DEAP) (Acros Organics) are dissolved in a diffracting suspension of polystyrene colloids. The total suspension is injected into a cell consisting of two quartz plates, separated by a 125-μm parafilm spacer. The cell is cooled in an ice bath and exposed to UV light from a Blak Ray (365 nm) mercury lamp to initiate polymerization. After 5 min of exposure, the cell was opened. The hydrogel usually adheres to one of the quartz plates. One of the quartz plates can be replaced with a plastic film with active acrylic groups attached to one surface (Bio-Rad). The gel covalently attaches to the plastic film during polymerization. The resulting hydrogel film bound to the substrate is washed in deionized water for 2 days.

We developed two methods to incorporate molecular recognition agents into the PCCA to produce IPCCA sensors. In the first method, molecular recognition agents that do not disrupt the crystalline order of the CCA are coupled to a polymerizable functional group. The polymerizable molecular recognition element is then dissolved in the CCA suspension along with the monomer, cross-linker, and photoinitiator. An intelligent copolymer IPCCA gel results after photopolymerization.

Utilizing this method, we incorporated the polymerizable crown ether acryloylamidobenzo-18-crown-6 (AAB18C6) into both AMD and NIPA-based PCCAs. This results in a gel that is sensitive to Pb^{2+}, Ba^{2+}, and K^+. In one example, we polymerized 2.11 mmol of AMD, 0.090 mmol of AAB18C6 (~4 mol % of the total monomer content), 0.072 mmol of bis-AMD (10% of the monomer weight), and 0.00720 mmol of DEAP dissolved in 3 mL of a 7 wt % suspension of polystyrene particles. A NIPA-based sensor with a response similar to that of Pb^{2+} was obtained using 1.37 mmol of NIPA, 0.149 mmol of AAB18C6, 0.070 mmol of bis-AMD, and 0.00720 mmol of DEAP.

Molecular recognition agents that disrupt the crystalline order of liquid CCA suspensions are incorporated into the PCCA by using a multistep process. Some of the amide groups in an acrylamide PCCA are hydrolyzed to acrylic acid groups. These carboxylic acid groups can then be coupled to a functional group on the molecular recognition agent (for example, to an -NH_2 group using a carbodiimide coupling agent) or to a second functional group that can then bind to the molecular recognition agent. Using the former method, we bound biotinamidopentylamine (Pierce) to the hydrolyzed gel using 1-[3-(dimethylamino)propyl]-3-ethylcarbodiimide hydrochloride (Aldrich) as a water-soluble coupling agent. The biotinylated gel then binds avidinated enzymes. We also bound the avidinated enzymes glucose oxidase (Pierce), and β-D-galactosidase (Pierce) to the biotinylated gel.

Sensor Testing. The IPCCA was exposed to solutions of varying analyte concentrations. The extinction spectra of the IPCCA were measured by a Perkin-Elmer Lambda-9 UV−visible−near-IR spectrophotometer at 1 min intervals. Upon exposure to analyte solutions, the IPCCA diffraction wavelength shifted to its equilibrium value, usually within 1−2 min. The diffraction peak did not further shift after 1−2 min for most samples. The sensor reached its equilibrium volume/color more slowly at low analyte concentrations, where the response was diffusion limited. For the temperature studies, the gel was cooled or heated to the desired temperature, and the extinction spectrum was measured by using an HP 8409 diode array spectrometer. Oxygen was excluded from the low-concentration glucose studies by N_2 purging, which also served to stir the solution. In all other experiments, the solution was not stirred.

Optrode Sensor. The fiber-optic probe tip was prepared utilizing a plastic sheet with active acrylate groups (Bio-Rad) as one wall of the cell described above. During polymerization, the IPCCA became chemically bonded to the active sites on the sheet. The plastic sheet was then cut into a small piece, which was affixed to the end of a bifurcated fiber-optic bundle. The bundle was dipped into a solution to determine the Pb^{2+} content. One of the bifurcated ends was coupled to the monochromator output of the Perkin-Elmer λ-9 absorption spectrophotometer, while the other end was coupled to its PMT input. The optrode was used as a dip probe; the spectrum of the light diffracted from the PCCA was measured to remotely determine the concentration of Pb^{2+} in solution.

Reactivity Studies. We studied the reactivity of AAB18C6 with NIPA and AMD. We photopolymerized linear polymers of AAB18C6 with NIPA or AMD, using DEAP as the inititator in water. We synthesized copolymers by reacting either 2.10 mmol of AMD with 0.09 mmol of AAB18C6 in 3 mL of water, or 2.13 mmol of NIPA with 0.21 mmol of AAB18C6 in 3 mL of water. The same concentrations of NIPA and AAB18C6 or AMD and AAB18C6 were used to synthesize the linear copolymers as were used to polymerize the IPCCAs. The linear copolymers were purified and dissolved in water for compositional analysis. The linear crown ether homopolymer is soluble in hot water and in acetone. The

NIPA copolymer was washed with hot water to remove any crown ether homopolymer, and the AMD copolymer was washed with acetone to remove any crown ether homopolymer. UV resonance Raman spectra of the copolymers of AAB18C6 with NIPA and AMD were measured, using 228.9-nm excitation from an intracavity frequency-doubled CW Ar^+ laser.[32] Raman measurements were made using 0.15 mW of 228.9-nm light, focused (~100 mm) onto the sample, in a rectangular quartz cell with a stirring bar. The Raman-scattered light was collected in the 135° backscattering geometry, dispersed by a Spex Triplemate monochromator, and detected by an intensified CCD (Princeton Instrument Co.). The accumulation time for each spectrum was 10 min.

The aromatic rings of AAB18C6 are strongly resonance enhanced by the 228.9-nm excitation. Sodium perchlorate (~932 cm^{-1}) was used as an internal standard to quantify the amount AAB18C6 in the copolymer solutions. The integrated peak areas were measured for the aromatic ring stretching band (1606−1609 cm^{-1}) and for the internal standard by curve-fitting using Galactic Industries's Grams 32 software.

RESULTS AND DISCUSSION

1. Theory. The IPCCA is a composite hydrogel. Hydrogels are cross-linked polymeric networks that are swollen with solvent. There is a significant body of literature which has examined the swelling phenomenon of hydrogels.[4−11,33−36,38−41] These networks change volume as their environment changes. Electrically neutral hydrogels swell into good solvents, and this tendency to swell is resisted by the elastic restoring force of the hydrogel network, which arises from the crosslinks. If a gel contains ionic groups fixed to the hydrogel polymers, the gel will swell more than will a corresponding nonionic gel in deionized water, due to a Donnan-type equilibrium established by the mobile counterions of the fixed charges inside the gel and by electrolytes in the gel or its bathing solution.[33−36] In addition, repulsions between charged groups will further swell the gel at high charge densities.

Our initial approach to understanding the IPCCA volume changes utilizes the standard hydrogel swelling theories elaborated by Flory and Tanaka.[33,36] The presence of the CCA and the high monomer and cross-linker densities in the IPCCAs may result in some discrepancy between these theories and the behavior of the IPCCA. However, as shown below, these theories do provide a basic insight into the IPCCA swelling phenomenon.

In these theories, the equilibrium hydrogel volume is determined by the sum of three energies: the free energy of mixing of the polymer chains with the solvent medium, the free energy of elasticity of the cross-linked network, and the ionic electrostatic energy due to the Donnan equilibrium and electrostatic repulsions between charged side groups on the polymer backbone:

$$\Delta F_{tot} = \Delta F_{mix} + \Delta F_{elas} + \Delta F_{ion} \qquad (1)$$

The polymer/solvent mixing and network elasticity terms have been derived by Flory[36] and Tanaka[33] as

$$\Delta F_{mix} = k_B T \frac{V}{\nu_{site}}(1-\phi)[\ln(1-\phi) + \chi\phi] \qquad (2)$$

and

$$\Delta F_{elas} = \frac{3k_B T}{2}\nu_e\left[\left(\frac{V}{V_0}\right)^{2/3} - 1 - \frac{1}{3}\ln\left(\frac{V}{V_0}\right)\right] \qquad (3)$$

respectively, where k_B is the Boltzmann constant, T is the temperature, and ν_{site} is the volume of a single lattice element in the Flory model.[34,36] ϕ is the polymer volume fraction in the swollen network, and χ is the Flory−Huggins polymer/solvent mixing parameter. ν_e is the effective number of polymer chains in the network, and V is the volume of the hydrogel in the presence of the analyte. We assume that V_0 is the volume of the hydrogel in pure water, since our PCCA does not swell in pure water after polymerization.

Hydrogels that do not contain ionizable or charged side groups on the polymer backbone do not change volume directly in response to the presence of ionic species in the solvent. For example, the cation-sensitive PCCA containing the AAB18C6 crown ether is a neutral gel in the absence of complexing cations. This gel does not change volume in response to electrolytes. However, if the crown ether complexes cations, the crown ether−cation complexes behave as ionized side chains; the formerly neutral gel becomes a polyelectrolyte gel.[38] The hydrogel then expands, primarily due to an osmotic pressure that arises from the mobile counterions, electrolytes, and fixed charges on the hydrogel. Repulsion between the crown ether−cation complexes will also cause the gel to swell, as will an increased solubility of the crown ether−cation side groups compared to the neutral, uncomplexed side groups (ΔF_{mix} would increase).[4−10,32−37]

Our preliminary calculations of polyelectrolyte PCCA swelling indicate that our gels swell primarily due to an increased osmotic pressure from a Donnan-type potential arising from the mobile counterions to the cation-complexed crown ethers on the gel backbone.[37] Tanaka et al. have shown that the degree of swelling of a polyelectrolyte gel is proportional to the number of ionic side groups per polymer chain in the gel (a polymer chain is defined as the length of polymer between cross-links).[34,35]

The PCCA already contains macroionic CCA colloidal particles. However, the charges on these particles have a very small impact on the gel volume. Although the colloidal particles in the IPCCAs contain ~2000 strong acid groups per particle, the number density of particles in the PCCA is only ~$10^{14}/cm^3$, which corresponds to only 1 ionic species per 100−200 chains of our typical PCCA. Tanaka et al. have shown that polyelectrolyte gels only begin to swell appreciably when there is one charge per 1−10 chains.[34,35] Thus, we observe little impact of the CCA colloidal particles on the gel swelling characteristics.

In contrast, our AMD IPCCA sensor with the largest dynamic range contains approximately 1 crown ether per 23 AMD monomers, where each chain comprises ~15 monomers. The best NIPA sensor contains 1 crown ether per ~10 NIPA monomers, with each chain comprising ~11 monomers.

Although it is appropriate to begin our investigation of the IPCCA swelling phenomenology in the context of the existing

(41) Koopman, J.; Hocke, J.; Gabius, H. J. *Biol. Chem. Hoppe-Seyler* **1993**, *374*, 1029.

polyelectrolyte gel swelling theory, we recognize that our high IPCCA cross-link density, the high concentration of crown ethers, and the presence of the colloids in the network are likely to result in discrepancies between our gel swelling characteristics and those predicted by the conventional gel swelling theories.

For an ionic gel, an imbalance in the concentration of mobile ions inside and outside the gel gives rise to an osmotic pressure, π_{osm}:[36]

$$\frac{\pi_{osm}}{N_A k_B T} = \left[\frac{ic_p}{z_-} - \nu_i(c_s^* - c_s)\right] \quad (4)$$

where i is the degree of ionization of the polymer's monomer units multiplied by the charge of the ionic group, c_p is the concentration of monomer units inside the gel, N_A is Avogadro's number, T is the absolute temperature, z_- is the valence of the counterelectrolyte, $\nu_i = \nu^+ + \nu^-$ is the sum of the cation and anion stoichiometries of the ionized $A_{\nu+}B_{\nu-}$ electrolyte, c_s^* is the concentration of mobile ions in the external solution bath, and c_s is the mobile ion concentration in the gel. In our crown ether containing IPCCA, the term ic_p (the concentration of ionized side groups in the gel multiplied by the their charge) corresponds to the product of the concentration of crown ether groups complexed to cations times the cation charge, $z^+[M^{z+}CR]$.

We initially assume that changes in the PCCA mixing free energy are small and are not significantly involved in the IPCCA volume expansion. Thus, the equilibrium swelling volume of the hydrogel is determined by the balance between the Donnan osmotic pressure arising from the fixed charged groups, π_{osm}, and the pressure arising from the elastic free energy:

$$\frac{\pi_{osm}}{RT} = \frac{z_+[M^{z+}CR]}{z_-} - \nu_i(c_s^* - c_s) = \nu_{ev}\left[\left(\frac{V_0}{V}\right)^{1/3} - \frac{1}{2}\left(\frac{V_0}{V}\right)\right] \quad (5)$$

where z_+ is the valence of the cation and ν_{ev} is the molar concentration of chains in the unswollen network.[36] At low analyte concentrations, the $(c_s^* - c_s)$ term is negligible. Thus, we expect that the volume swelling at low analyte concentrations, calculated as $(V_0/V)^{1/3} - 0.5(V_0/V)$, should be proportional to the concentration of mobile counterions of the fixed charges in the IPCCA.

The concentration of crown ether-bound Pb^{2+} $[Pb^{2+}CR]$ ionic groups is

$$[Pb^{2+}CR] = \frac{K[Pb^{2+}][CR_0]}{1 + K[Pb^{2+}]} \quad (6)$$

where $[Pb^{2+}]$ is the Pb^{2+} concentration in the gel (identical to that of the bath at equilibrium) and $[CR_0]$ is the total concentration of crown ethers in the IPCCA. Combining eqs 5 and 6 and neglecting $(c_s^* - c_s)$ yields

$$2[Pb^{2+}CR] = \frac{2K[Pb^{2+}][CR_0]}{1 + K[Pb^{2+}]} = z_-\nu_{ev}\left[\left(\frac{V_0}{V}\right)^{1/3} - \frac{1}{2}\left(\frac{V_0}{V}\right)\right] \quad (7)$$

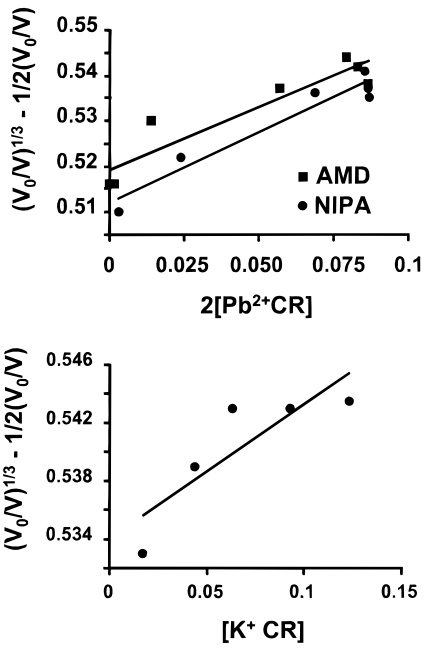

Figure 3. Dependence of the elastic pressure volume term, $(V_0/V)^{1/3} - {}^1/_2[V_0/V]$ on $z_+[M^{z+}CR]/z_- = 2[Pb^{2+}CR]$ or $[K^+CR]$. The slopes should equal $(z_-\nu_{ev})^{-1}$. The slope of the NIPA IPCCA Pb^{2+} and K^+ response curves are both 0.4 M^{-1}, giving $z_p\nu_{ev}$= 2.5 M. The slope of the AMD IPCCA Pb^{2+} response curve is 0.37 M^{-1} giving $z_-\nu_{ev}$= 2.7 M. This compares to $z_-\nu_{ev}$ values we naively calculate from the initial monomer and cross-linker concentrations of 0.046 and 0.048 M for the AMD and NIPA IPCCAs, respectively. The highest concentration data were not used in calculating the slopes.

Figure 3 shows the mobile counterion concentration dependence of the elastic pressure restoring term as calculated from the change in diffracted wavelength $(d/d_0)^3 = (\lambda/\lambda_0)^3 = V/V_0$, for the NIPA and AMD IPCCAs in Pb^{2+}, and for the NIPA IPCCAs in K^+. $[M^{z+}Cr]$ was calculated assuming an infinite bath volume, so that $[M^{z+}]$ is constant. The data in Figure 3 were obtained at conditions approaching an infinite bath containing Pb^{2+}or K^+.

At high Pb^{2+} concentrations (>1 mM) or high K^+ (10 mM), where nearly all of the crown ethers in the IPCCA are complexed to Pb^{2+} or K^+, $z(c_s^* - c_s)$ becomes large enough to reduce the Donnan potential of the hydrogel. This decreased gel volume compared to that predicted by eq 7 may account for the deviation from linearity seen at the highest concentrations.

The slope of the data in Figure 3 should equal $z_+/(z_-\nu_{ev})$. The molar concentrations of "effective" polymer chains, ν_{ev}, obtained from the Pb^{2+} and K^+ volume response curves for the NIPA IPCCA were both 2.5 M. Assuming 100% conversion of the monomers and cross-linkers during polymerization, the ν_{ev} value should, theoretically, be much smaller, 0.046 M for the NIPA IPCCA. Similarly, the Pb^{2+} volume response curve of the AMD IPCCA gives a too-high $z\nu_{ev}$ value of 2.7 M, compared to the expected 100% conversion value of 0.048 M. Thus, the IPCCA is calculated to possess a much higher concentration of chains than can be accounted for by the gel composition.

We estimate that there should be one cross-link for every two chains. Thus, the data in Figure 3, in the context of eq 7, indicate ~25-fold more cross-links than can be calculated from the gel composition. This discrepancy probably results from the presence of the CCA colloidal particles in the hydrogel. The presence of

inert fillers in rubber, for example, decreases the elasticity of the network nonlinearly in proportion to the volume fraction of filler.[36] Fillers that interact with the hydrogel polymer via adsorption, chemisorption, or covalent bonding decrease the elasticity of networks by acting as additional cross-link points.[36] We have observed through EPR spin probe labeling studies that acrylamide polymers strongly adsorb to the CCA polystyrene colloids.[37] We also measured the Young's modulus of the PCCA acrylamide gels and similar acrylamide gels without the embedded CCA. The embedded CCA increased the Young's modulus by a factor of ~4. These data indicate that the morphology, and hence the elasticity, of the IPCCA network significantly differs from the elasticity described by simple hydrogel theory. Furthermore, we use a large cross-linker density, which will result in short chains whose end-to-end distances are not described by the Gaussian distribution assumed by the standard hydrogel theory.[54] A network of short chains will also have a lower elasticity than that predicted by eq 3.

2. Crown Ether IPCCA Response. We have characterized the IPCCA's response to analytes and interferences. We examined the sensor's ability to detect ionic species that are strongly complexed by the crown ether. We also examined the response of the IPCCA to weakly complexed cations (section 2.1). We examined the effects of ionic strength and anion type on the response to analytes (sections 2.2 and 2.3). We also examined the effects of solvent and temperature on the response of the gel (sections 2.4 and 2.5). Finally, in section 2.6, we characterized the dependence of the response of IPCCAs upon the gel acrylamide and cross-linker composition.

It is important to note that the sample solution analyte concentrations can be depleted by reacting with or binding to the recognition elements for large IPCCA volumes and/or for low volumes of sample solutions and/or for low analyte concentrations. In these cases, the analyte concentration will not remain constant during exposure of the sample solution to the IPCCA sensor; this will quantitatively affect the expectations of eq 7.

2.1. Detection of Analytes. The response of the IPCCA sensor containing the crown ether AAB18C6 to Pb^{2+}, Ba^{2+}, or K^+ is a function of the concentration of those species in the medium surrounding the PCCA. The polymerized AAB18C6 crown ether groups strongly complex these ions.[35−37] As the concentration of these analytes in the gel environment increases, an increased fraction of crown ethers bind analyte cations, which causes the gel to swell. The wavelength diffracted from the IPCCA sensor sensitively monitors the gel's linear dimension and hence its volume. Although the degree of swelling is not linear with respect to the cation concentration, the response is reproducible, and a calibration plot can be used to determine analyte concentrations from the wavelength diffracted from the sensor. Figure 4 shows the calibration plots for the AMD and NIPA crown ether-based IPCCA sensors described above for Pb^{2+}, while Figure 5 shows the calibration plot of the NIPA crown ether-based sensor for K^+. The diffraction wavelength shift for 1 mM Pb^{2+} is 3.5-fold larger than that for K^+. The swelling volume change is thus 42-fold larger for Pb^{2+} than that for K^+. The response to Ba^{2+} is within 2 nm of the diffraction shift for the same concentration of Pb^{2+} (not shown).

The crown ether complexes metal cations, with an affinity that depends on both the cation's radius and its charge.[34−36] AAB18C6 binds Pb^{2+}, Ba^{2+}, and K^+ most strongly. The parent crown ether, 18-crown-6, shows binding constants of 18 600, 7400, and 107 M^{-1},

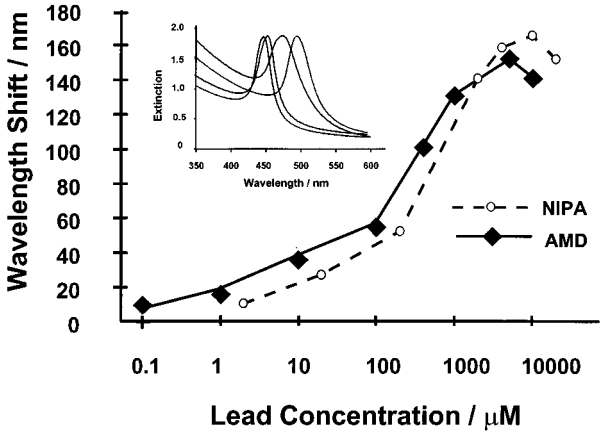

Figure 4. Response of the AMD 5 mol % AAB18C6 and the NIPA 10 mol % AAB18C6 IPCCA (~12% crosslinker) sensors to $Pb(NO_3)_2$. The shift in the diffracted wavelength is relative to the wavelength diffracted in pure water. Inset shows the extinction spectra of the AMD sensor in water for 0.1, 10, and 100 μM Pb^{2+}.

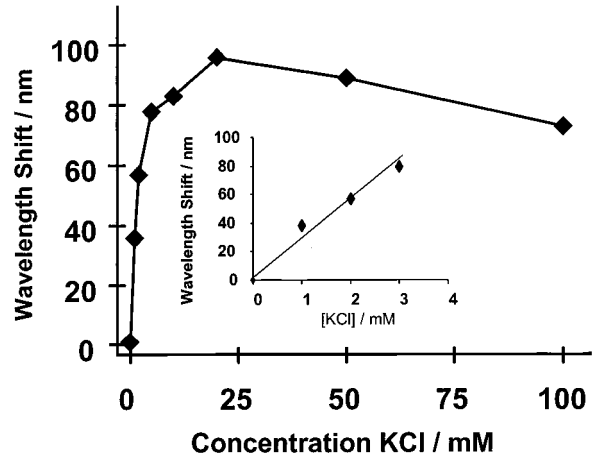

Figure 5. Response of the 10 mol % AAB18C6 NIPA IPCCA sensor to K^+. The sensitivity for K^+ detection is ~3 orders of magnitude less than that for Pb^{2+}. The inset shows the low K^+ concentration response.

(42) Lamb, J. D.; Izatt, R. M.; Christiansen, J. J.; Eatough D. J. In *Coordination Chemistry of Macrocyclic Compounds*; Melason, G. A., Ed.; Plenum Press: New York, 1979; Chapter 3, p 145.
(43) Izatt, R. M.; Terry, R. E.; Nelson, D. P.; Chan, Y.; Eatough, D. J.; Bradshaw, J. S.; Hansen, L. D.; Christiansen, J. J. *J. Am. Chem. Soc.* **1976**, *98*, 7626.
(44) Kopolow, S.; Hogen Esch, T. E.; Smid, J. *Macromolecules* **1973**, *6*, 133.
(45) Mukae, K.; Sakurai, M.; Sawamura, S.; Makino, K.; Kim, S. W.; Ueda, I.; Shirahama, K. *J. Phys. Chem.* **1993**, *97*, 737.
(46) Wong, L.; Smid, J. *Polymer* **1980**, *21*, 195.
(47) Agostiano, A.; Caseli, M.; Della Monica, M. *J. Electroanal. Chem.* **1976**, *74*, 95.
(48) Asfari, Z.; Vicens, J. *Acros Org. Acta* **1996**, *1*, 18.
(49) Asfari, Z.; Vicens, J. *Acros Org. Acta* **1996**, *2*, 8.
(50) Kubo, Y.; Maeda, S.; Tokita, S.; Kubo, M. *Nature* **1996**, *382*, 522.
(51) Savage, M. D.; Mattson, G.; Desai, S.; Neilander, G. W.; Morgensen, S.; Conklin, E. J. *Avidin-Biotin Chemistry: A Handbook*; (Pierce Chemical Co.: Rockford, IL, 1992.
(52) Raba, J.; Mottola, H. *Crit. Rev. Anal. Chem.* **1995**, *25*, 1.
(53) Bright, H. J.; Porter, D. J. T. *The Enzymes, Vol. XII*, 2nd ed.; Academic Press: New York, 1975; Chapter 7, p 421.
(54) Mark, J. E. *Adv. Polym. Sci.* **1982**, *44*, 1.

respectively; 18-crown-6 ether shows much weaker affinities for other cations. The crown ether−metal interaction increases with increasing cation charge. We experimentally observe Pb^{2+} and Ba^{2+} detection limits below 0.1 μM (∼ 40 ppb Pb^{2+}), while the detection limit for K^+ is ∼1 mM. The bath volume at the lowest concentrations of Pb^{2+} must be very large compared to the IPCCA volume in order for the sensor to reach its equilibrium volume at the original analyte concentration. At low concentrations, the IPCCA concentrates Pb^{2+}, for example, and depletes the bath Pb^{2+} concentration.

We observe that, above ∼5 mM Pb^{2+} concentration, the gel shrinks with increasing Pb^{2+} concentration (Figure 4). Using the Pb^{2+} complexation equilibrium constant of ∼18 600 M^{-1}, we calculate that essentially all gel crown ethers bind Pb^{2+} at ∼5 mM if the sample solution is large. The gel-bound crown ethers should also be saturated in ∼20 mM K^+ solutions, assuming an equilibrium constant of ∼107. Thus, the saturation of the analyte response of these IPCCA results from saturation of the IPCCA crown ether recognition groups. We can increase the dynamic range of these IPCCA by increasing the polymer density of the IPCCA; this maintains the relative concentrations of crown ether to acrylamide chains. We can fabricate IPCCA for use at higher analyte concentrations by using recognition agents with smaller equilibrium binding constants.

2.2. IPCCA Response to Interfering Cations. The sensitivity and selectivity of the sensor are primarily determined by the binding constant and selectivity of the recognition agent. The crown ether AAB18C6 weakly binds cations other than Pb^{2+}, Ba^{2+}, and K^+. For example, the 18-crown-6 binding constant for Na^+ complex is 6.3 M^{-1}, compared to values of 107, 7400, and 18 600 M^{-1} for K^+, Ba^{2+}, and Pb^{2+}, respectively.[35]

The swelling of the gel is a function of the number of crown ethers complexed to cations. A lower binding constant means that a higher concentration of analyte is necessary to attain a given concentration of complexed crown ether in the gel. However, at higher electrolyte concentrations, the Donnan potential that drives the gel swelling decreases. This means that, as the crown ether binding constant decreases, the maximum diffraction shift at high analyte concentrations will decrease, and the detection limit will increase. For example, the NIPA sensor's maximum diffracted wavelength shifts in response to Pb^{2+}, K^+, and Na^+ are ∼165 (10 mM), ∼96 (20 mM), and ∼39 nm (100 mM), respectively. Ca^{2+} should have a constant for binding to AAB18C6 similar to that of as Na^+; the NIPA sensor swelled by 32 nm in response to ∼100 mM Ca^{2+}.

Cations with negligible binding constants have very little effect on the sensor. H^+ and Li^+ are too small to complex to more than a few of the oxygens in 18-crown-16, while Cs^+ is too large to fit into the cavity.[35] Figure 6 shows the shifts in the diffraction, relative to the diffraction in pure water for various concentrations of NaCl, $CaCl_2$, LiCl, and CsCl.

Cs^+ causes the diffraction wavelength to red-shift by 21 nm at a 1 mM concentration. At higher Cs^+ concentrations, the diffraction wavelength begins to decrease, finally falling below the original diffraction wavelength at 40 mM. In 200 mM CsCl, the diffraction wavelength of the sensor was 59 nm below that of the sensor in pure water. Although Cs^+ is too large to fit into the crown ether cavity, it can complex to 18-crown-6 while remaining

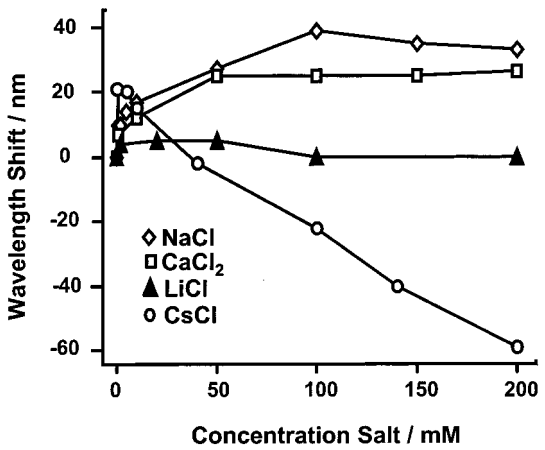

Figure 6. Response of the 10 mol % AB18C6 NIPA gel (10 wt % cross-linker) to various cations in the absence of Pb^{2+} and K^+. Li^+ is not complexed, while Na^+ and Ca^{2+} are weakly complexed. Cs^+ appears to form a 2:1 complex; CsCl solutions above 1 mM cause the IPCCA to shrink. See text for details.

out of the plane of the oxygen atoms. Ce^+ forms 2:1 sandwich complexes with polymeric crown ethers.[44] Crown ethers that are spaced along the same polymer chain at optimal distances to form sandwich complexes should have the greatest affinities for Cs^+. These sites fill first, accounting for the swelling at the lowest Cs^+ concentration. Crown ethers from different chains begin complexing Cs^+ at higher concentrations. Those that form sandwich complexes cause the IPCCA to contract because they act as effective cross-links to increase the number of cross-links, which increases the elastic restoring pressure of the network (eq 7).

2.3. IPCCA Response to Noncomplexing Electrolytes. The swelling of the cation-sensitive IPCCA decreases with increasing ionic strength for a given concentration of complexed ion. The osmotic pressure due to the Donnan equilibrium decreases with an increasing ionic strength. Figure 7 shows the response of the IPCCA at 500 μM Pb^{2+} to increasing LICl concentrations.

High salt concentration will also favor formation of tight ion pairs with the crown ether−cation complexes, which will reduce the net charge on the polymer. In contrast, in the absence of Pb^{2+}, the gel is neutral and does not change volume in response to Li^+ (Figure 6).

2.4. IPCCA Response to Anions. The net charge localized on the cation-complexed crown ether complex depends on the identity of the anions in solution, as well as on the solution ionic strength.[44,46] The complexed cation's counterion may form an ion pair to reduce the effective charge. Figure 8 compares the response of the crown ether PCCA to 5 mM KCl, 5 mM KOH, 2.5 mM K_2CO_3, and 2.5 mM K_2HPO_4. The IPCCA swells nearly identically in 5 mM KOH and KCl, while the diffraction wavelength shift in 2.5 mM K_2CO_3 and K_2HPO_4 differs by as much as 10 nm from the response to KCl (Figure 8). The divalent anions would be expected to more easily form ion pairs to reduce the swelling of the sensor.

2.5. PCCA Response to Nonaqueous Solvents. Environmental factors can both affect the volume of the hydrogel and influence the molecular recognition process. Changes in solvent are well known to cause changes in the equilibrium hydrogel volumes. For example, changing the solvent composition changes

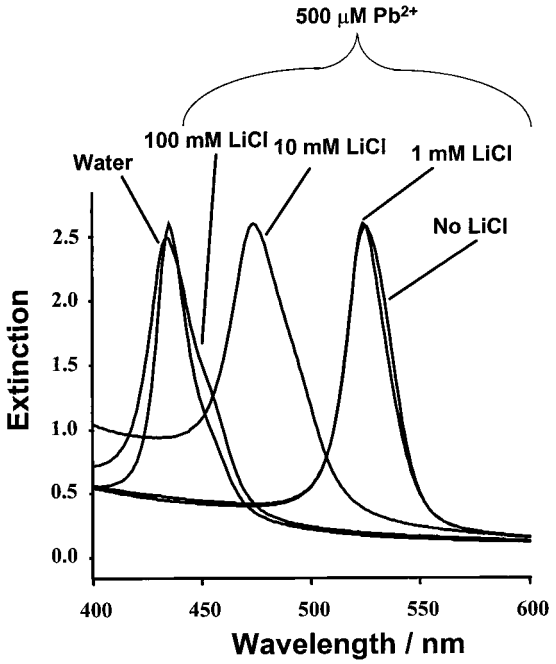

Figure 7. Response of the 10 mol % NIPA sensor to 500 μM Pb^{2+} for varying LiCl concentrations. The diffraction peak in pure water is also shown for reference.

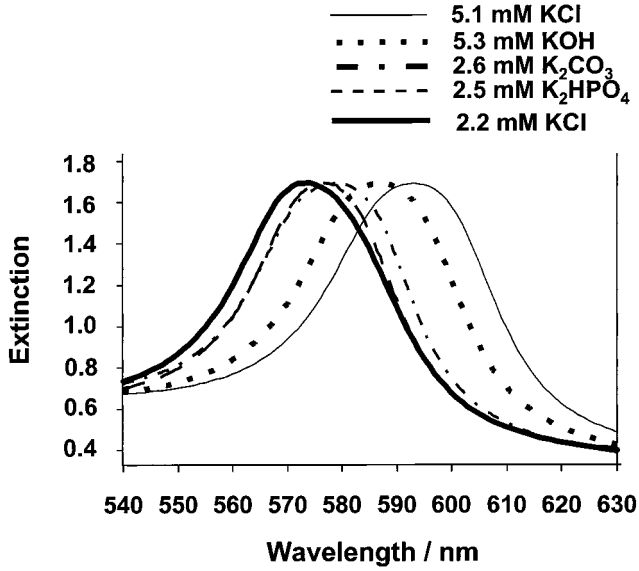

Figure 8. Response of the 10 mol % AAB18C6 NIPA sensor to 5 mM K^+ in the presence of different anions. The response to 2.2 mM KCl is also shown for reference. The IPCCA diffraction band maximum is at 510 nm in pure water.

the free energy of mixing by changing the Flory–Huggins polymer/solvent interaction parameter, χ.[33–40]

We examined the effect of moderate concentrations of methanol on the IPCCA sensor response. Most hydrogels shrink with increasing methanol concentration. However, NIPA and other alkyl-substituted acrylamides are known to exhibit re-entrant phase behavior (cononsolvency) in methanol/water mixtures; NIPA networks are swollen in pure water or pure methanol but collapse in mixtures of the two solvents.[40] In 20 vol % aqueous methanol, the 10 mol % AAB18C6 NIPA IPCCA diffraction blue-shifts 20 nm relative to that in pure water. However, the IPCCA diffraction in

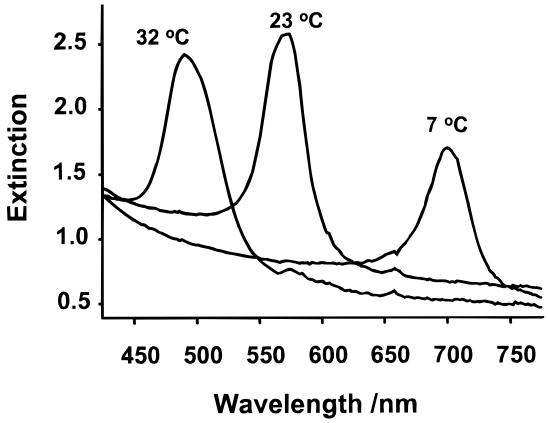

Figure 9. Temperature dependence of diffraction of the NIPA 10 mol % AAB18C6 IPCCA sensor in the presence of 5 mM KCl. The spectra were measured using an HP diode array spectrometer.

the presence of 5 mM KCl is red-shifted by ~50 nm relative to the diffraction that occurs in an aqueous 5 mM KCl solution.

This increased swelling probably results from an increased affinity of the crown ether for K^+ in 20% methanol. In order to complex with the crown ether, the cation's solvation sphere must be disrupted. As the solvent polarity decreases, it becomes easier to remove the solvation sphere, which increases the equilibrium constant for metal/crown ether complexation.[41–47] The increased complexation constant causes the gel to swell more in the 20% methanol solution (5 mM KCl) than in aqueous 5 mM KCl. However, for a 30% methanol solution containing 5 mM KCl, we observe less swelling than in pure water containing 5 mM KCl. Although the crown ether has a higher affinity for K^+ in 30% methanol than in water, the NIPA polymer is much less soluble in 30% methanol than in 20% methanol, and the hydrogel swells less.

2.6. IPCCA Response to Temperature Alterations. The volume of AMD hydrogels does not significantly depend on temperature; however, temperature dramatically impacts the swelling of some hydrogels.[2] For example, NIPA gels are highly sensitive to changes in temperature; pure NIPA gels undergo a volume phase transition and collapse to a minimum volume between ~31–35 °C, depending on the exact gel composition.[34,35] Our NIPA sensor collapses at ~39 °C. Figure 9 shows the temperature dependence of the NIPA IPCCA diffraction in the presence of 5 mM KCl.

At 32 °C, the NIPA sensor does not swell for KCl concentrations between 5 and 50 mM. However, swelling is observed at higher KCl concentrations; the diffracted wavelength red-shifts by 40 nm between 50 and 100 mM KCl. This may be due to a decreased equilibrium constant for crown ether complexation of K^+ with increasing temperature.[42] At ~39 °C, the NIPA sensor does not respond to the KCl at any concentration. The dynamic range of AMD IPCCAs also shifts to a higher concentration region at 32 °C, which is likely due to a decrease in the crown ether–cation binding constant with increasing temperature.[42,43] Thus, the working concentration range of the IPCCA sensors can be controlled by controlling the temperature.

2.7. Dependence of IPCCA Response to Variations in Hydrogel Composition. The gel polymer composition also determines the extent of IPCCA swelling. For example, Figure

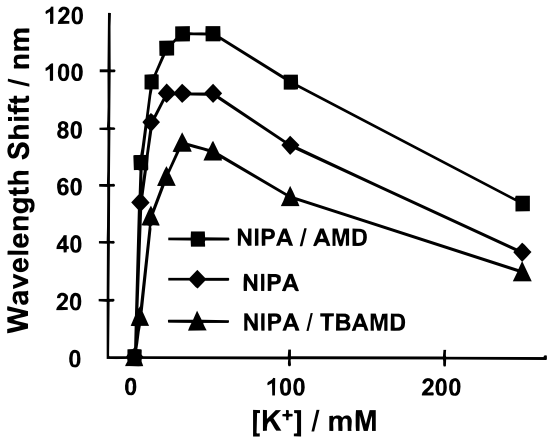

Figure 10. Response of 10 mol % AAB18C6 IPCCA sensors to varying acrylamide gel compositions. NIPA, *N*-isopropylacrylamide; AMD, acrylamide; and TBAMD, *tert*-butylacrylamide. All IPCCAs contained 10 mol % cross-linker.

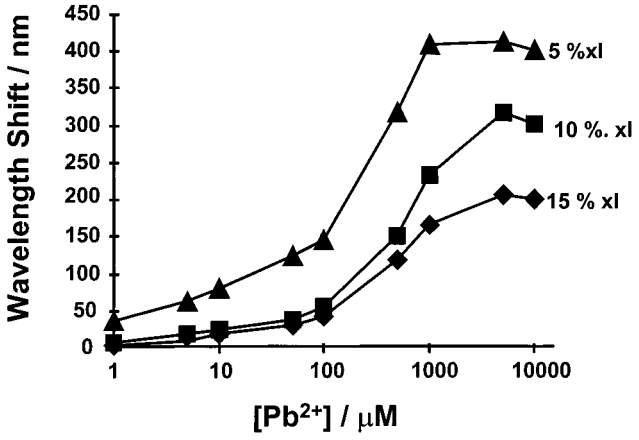

Figure 11. Cross-link density dependence of Pb^{2+} response of the NIPA 10 mol % AAB18C6 IPCCA. The wavelength shift is relative to the diffraction in pure water, ~450 nm.

10 shows the response of IPCCA sensors made from NIPA and AAB18C6, copolymerized with other acrylamide monomers. All of these sensor gels contained 10 mol % AAB18C6. The lowest responsivity IPCCA was a 70 mol % NIPA, 30 mol % *tert*-butylacrylamide hydrogel (TBAMD); a pure NIPA gel showed intermediate responsivity, while a 70 mol % NIPA, 30 mol % AMD gel showed the greatest responsivity. The affinity of the crown ether for K^+ should be independent of acrylamide composition; all three gels showed maximum swelling at ~20−25 mM KCl concentrations. However, the magnitude of swelling in response to a given KCl concentration depended on the gel acrylamide composition.

The amount of crown ether in the IPCCA determines the sensitivity and detection range of the material. The gel is a copolymer network. The physical properties of the network are determined by the ratio of acrylamide monomers to crown ether-bearing monomers. The most sensitive AMD-based cation sensor contained ~5 mol % AAB18C6. Decreasing the AAB18C6 content from 5 to 3 mol % increased the detection limit of Pb^{2+} from ~0.1 to ~50 μM. The dynamic range also decreased from 0.1 μM−5 mM for the 5 mol % AAB18C6 material to 50 μM−1 mM for the 3 mol % AAB18C6 IPCCA. Increasing the AAB18C6 content from 5 to 10 mol % also reduced the dynamic range and increased the Pb^{2+}detection limit. We found that the optimum AAB18C6 content in the NIPA IPCCA was ~10 mol %.

The reactivity of AMD and NIPA toward AAB18C6 determines the amount of crown ether groups incorporated into the gel from a given feed of monomers in the pregel solution. The monomer feed of the best NIPA sensor contained 10 mol % AAB18C6, while the best AMD sensor's monomer feed contained 5 mol % AAB18C6. Using UV Raman spectroscopy, we determined the reactivity of AAB18C6 with AMD and NIPA. We copolymerized AAB18C6 with NIPA or AMD in water, using the same concentration of polymerizable crown ether and comonomer used to polymerize the IPCCAs. The copolymer was purified, and the concentration of AAB18C6 was determined by monitoring the intensity of the aromatic ring band at ~1609 cm^{-1}. The ratio of crown ether in the monomer feed to crown ether in the polymer was ~1.5 times greater in the AMD copolymer than in the NIPA copolymer. Thus, AMD has a higher reactivity ratio with respect to AAB18C6.

The number of cross-links in the hydrogel determines the IPCCA elasticity, which determines the volume response (eq 7). Figure 11 shows the effect of cross-link density on the IPCCA volume response to Pb^{2+}. The bis-AMD cross-linker concentration was varied while maintaining all other components constant. Decreasing the cross-linker content increased the swelling, as expected from eqs 3, 5, and 7, which indicate that the degree of swelling should be inversely proportional to the cross-link density. However, we observe less than a 3-fold increase in swelling of the 5% cross-linker IPCCA compared to that with the 15% cross-linker IPCCA. This may be due to the contribution of the CCA network to the effective cross-linker density, as discussed above.

3. Enzyme IPCCA. We also fabricated IPCCA sensors using biological molecular recognition elements. We incorporated enzymes into the gel using the biotin−avidin interaction. Although enzymes can be incorporated into hydrogels using entrapment, we were unable to dissolve enzymes into the diffracting PCCA precursor suspension/solution without destroying the CCA crystalline order. However, we were able to attach both avidinated galactosidase and avidinated glucose oxidase onto a biotinylated gel.[51] The galactosidase was determined to be active after binding by its reaction with *o*-nitrophenol galactoside and the appearance of free *o*-nitrophenol absorption at 405 nm. The glucose oxidase was determined to be active from the increase in ionic strength of a glucose solution exposed to the sensor, due to production of gluconic acid.

3.1. PCCA Response to Enzyme Substrates. The sensors respond to 0.1−0.5 mM solutions of galactose or glucose. Figure 12a shows the response of the galactose sensor, and Figure 12b shows the response of the glucose sensor to varying concentrations of galactose or glucose. Neither sensor responded to sucrose nor to the substrate of the other enzyme (glucose or galactose). The galactose sensor gradually ceased to function over a 2-month period, but the glucose sensor has continued to function for over 6 months.

Glucose oxidase converts glucose to gluconic acid in a two-step process. In the first step, glucose is converted to gluconic acid, and the enzyme is reduced. In the second step, the enzyme is reconverted to its oxidized form by oxygen in the solution,

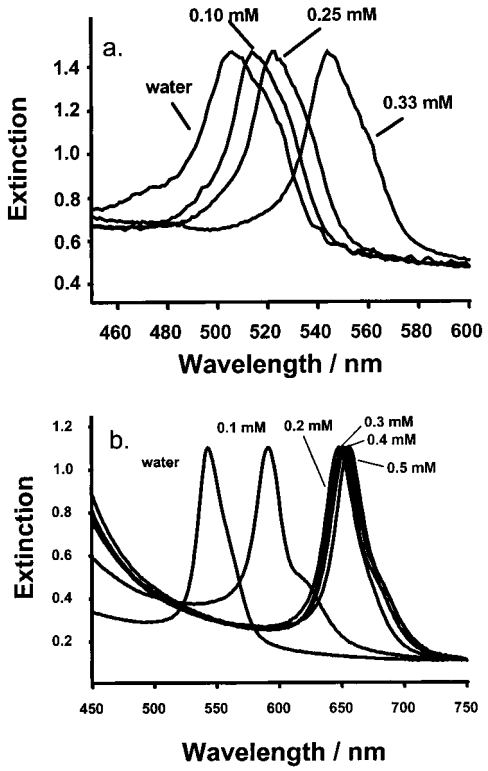

Figure 12. (a) Response of the IPCCA sensor containing galactosidase to galactose. (b) Response of the IPCCA containing glucose oxidase to glucose.

producing H_2O_2 as a byproduct:[52,53]

$$\text{enzymeH(ox)} + \text{glucose} \rightarrow \text{enzyme}^-\text{(red)} + \text{gluconic acid} + \text{H}^+$$

$$\text{H}^+ + \text{enzyme}^- \text{(red)} + \text{O}_2 \rightarrow \text{H}_2\text{O}_2 + \text{enzyme(ox)}$$

The production of the reduced anionic species in the intermediate step appears to cause the glucose sensor swelling. When the sensor is placed in a glucose solution of limited volume (~1−10 times the sensor volume), the sensor swells initially (~15 min) and then shrinks as the glucose is consumed and its concentration decreases. However, if the solution is first deoxygenated, the sensor swells but does not shrink over time, and the ionic strength of the solution does not increase with time. At very low levels of oxygen, where the regeneration rate of the oxidized enzyme is vanishingly small, the IPCCA sensor swells in subnanomolar concentrations of glucose. We observed a 30-nm diffraction wavelength shift in 10^{-10} M glucose within 20 min and an 8-nm wavelength shift in 10^{-12} M glucose within 30 min when the bath was deoxgenated with N_2 and stirred. In the presence of oxygen, no wavelength shift occurs for 10^{-12} M glucose. This indicates that the intermediate form of the enzyme is the source of the diffracted wavelength shift.

Sparging N_2 through the solution does not completely exclude oxygen from the solution. In the total absence of oxidizer, the sensor should eventually reach its maximum volume if the bath solution contains only one stoichiometric amount of glucose relative to the glucose oxidase in the gel. In principle, we could

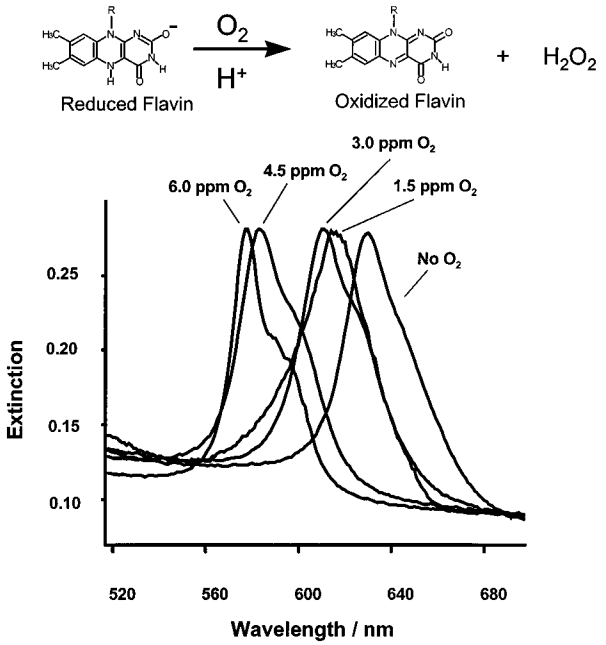

Figure 13. Response of the glucose oxidase containing IPCCA to oxygen in the presence of a constant 0.2 mM glucose concentration.

detect diffraction from a 1-μm^3 IPCCA sensor. Since the glucose oxidase concentration in our IPCCA is ~10^{-4} M, and since we can detect a ~10-nm shift in diffraction, this suggests a detection limit of less than the ~10^6 molecules of glucose which would be required to fully reduce the glucose oxidase in this 1 μm^3 IPCCA.

The glucose sensor does not swell in glucose solutions containing >0.2 mM electrolytes, which indicates that the swelling we observe is due to the formation of ionic species in the gel, since the osmotic pressure due to the fixed ionic charges in the gel will be reduced by the presence of electrolytes in the gel bath (eq 5).

3.2. Enzyme IPCCA Response to Oxygen. We can utilize the oxidation of glucose oxidase to determine the dissolved oxygen concentration. We immersed the glucose IPCCA sensor in baths of 0.2 mM glucose at varying oxygen concentrations. In the absence of oxygen, the sensor diffraction red-shifts by 85 nm at 0.2 mM glucose. Figure 13 shows the response of this IPCCA to oxygen. Increasing oxygen concentration blueshifts the diffraction wavelength due to the shift in the steady state toward a lower concentration of the reduced, anionic enzyme.

4. IPCCA Response Rates. The 125 μm-thick IPCCA sensors reach their equilibrium volume in 10 mM K^+ or 10 mM Pb^{2+} in less than 30 s but reach equilibrium more slowly in submillimolar Pb^{2+} solutions. The equilibrium response can also be limited by the bath volume at concentrations due to the uptake of large quantities of Pb^{2+} by the IPCCA, which significantly depletes the analyte species in small sample volumes.

The biosensors reach their equilibrium volumes in ~1 min. The response of both sensors is determined by the mass transport of substrate into the gel. In addition, the biosensor's response is limited by the rate of enzyme reaction. Decreasing the thickness of the sensor decreases the response time. We observe that a ~10-μm-thick IPCCA reaches its equilibrium volume in milliseconds; diffraction from this gel is sufficiently intense to be easily visible to the naked eye.

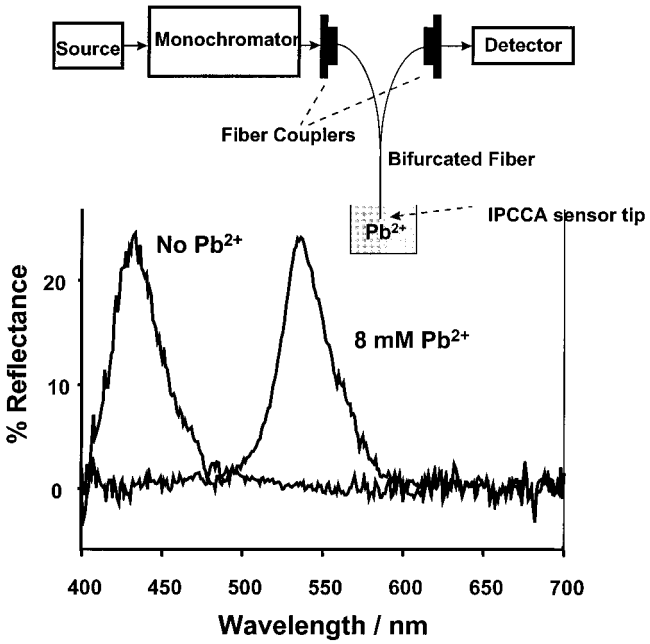

Figure 14. Reflectance spectra from the optrode IPCCA sensor in pure water and in 8 mM Pb^{2+}. The IPCCA fixed to the fiber tip contained ~20 wt % cross-linker relative to the total monomer content and was polymerized on an plastic sheet with acrylic groups on its surface. The spectra were measured using the Perkin-Elmer λ-9 absorption spectrophotometer, coupled to a bifurcated optical fiber.

5. IPCCA Optrode Sensor. We polymerized the IPCCA sensor containing AAB18C6 and 20% cross-linker onto a plastic film and attached a small portion of this film to the end of a bifurcated fiber optic. The fiber optic was coupled to a Perkin-Elmer λ-9 absorption spectrophotometer, as described above. Using this optrode as a dip probe, we remotely measured the diffracted wavelength shift in an 8 mM Pb^{2+} solution. The sensor reached equilibrium volume within 1 min. Figure 14 shows the experimental design of the optrode sensor and reflectance spectra from the sensor in a 8 mM Pb^{2+} solution and in pure water. This is obviously a viable approach for remote measurements.

Based on the work discussed above, we should be able to fabricate IPCCA sensors for a host of different analytes. These IPCCA sensors could be fabricated into an array of optrode sensors by placing the different IPPCCA sensors onto different fibers in a fiber-optic bundle; this bundle could be examined in real time to quantify multiple analytes. We would utilize IPCCA sensors with overlapping sensitivities but with differential responses to the analytes and the interfering species. Thus, we would be able to combine the information from the swelling responses of these different IPCCAs to determine the concentration of the different analytes. For example, we were able to utilize two IPCCAs to determine the concentration of dilute Pb^{2+} in millimolar solutions of interfering LiCl. The presence of millimolar concentrations of LiCl reduced the IPCCA sensor's Pb^{2+} response. We separately measured the concentration of LiCl using a hydrolyzed acrylamide PCCA that nonselectively shrinks in response to the presence of any ionic species.[38−40] Calibration curves for the Pb^{2+} response of the IPCCA can be determined for different concentrations of interfering LiCl (Figure 15).

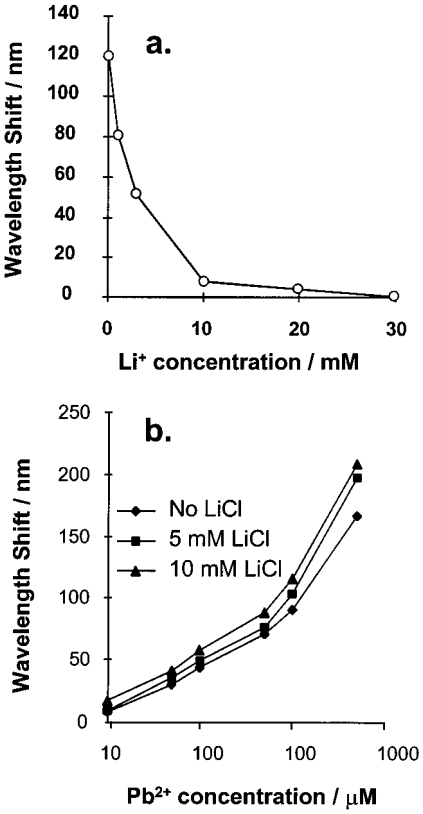

Figure 15. (a) Response of hydrolyzed gel to varying concentrations of LiCl. The wavelength shift is relative to the diffracted wavelength in pure water. (b) Response of 10 mol % NIPA IPCCA (6% cross-linker) to Pb^{2+} in 5 and 10 mM LiCl solutions. The LiCl concentration is determined from the diffraction of the hydrolyzed PCCA, which is used to choose the correct Pb^{2+} calibration curve.

Determination of the LiCl concentration then allows us to choose the correct Pb^{2+} calibration curve. Our future work will further demonstrate the utility of these parallel detection schemes.

CONCLUSIONS

We have demonstrated the utility of IPCCAs as sensor materials. The IPCCAs demonstrated here are a new motif for fabricating sensors. The utility of this motif is limited only by the availability of suitable molecular recognition agents. For example, we can imagine binding TB, cancer cell, or HIV antibodies to the gel for diagnostic sensors. Arrays of sensors could test for interferences or for multiple analytes within the same sample. As we have demonstrated, the material can be coated onto optical fibers so that these sensors can remotely measure analytes in hazardous environments, or even in vivo.

Incorporating chemical recognition agents with more selective recognition chemistry (e.g., calixarenes[48−50]) with large equilibrium constants for complexation to particular ionic species will improve the sensitivity and selectivity of the sensors. In order to eliminate interference from nonspecific interactions, several sensors with different responsivities to environmental interferences could be combined to deconvolute interferences.

These sensors have the great advantage of having a response which is easily detectable by the human eye. Pb^{2+} concentrations as low as 400 ppb can be visually detected by the diffraction

wavelength shift without the aid of a spectrometer. The sensitivity and detection range of these sensors be tailored by controlling the gel composition, as well as the molecular recognition agents used.

The swelling mechanisms for both the cation and glucose sensors involve formation of ionic groups on the polymer chains of the hydrogel, due to cation binding or the reduction of an enzyme. We are also currently developing sensors that change volume in response to nonionic molecular recognition processes, such as antibody/antigen interactions. We envision applications in medicine, environmental chemistry, process control, and remote sensing for these unique materials.

ACKNOWLEDGMENT

We thank Ms. Maria Kurnikova, Prof. Rob C. Coalson, and Prof. Stephen G. Weber for helpful discussions, and Prof. Weber and Mr. Mark Stouffer for use of the HP diode array spectrometer. This work was supported by the Office of Naval Research, Grant N00014-94-10-0592, AFOSR AASERT Grant F 49620-94-1-0268, and National Science Foundation Grant CHE-9633561.

Received for review August 8, 1997. Accepted November 21, 1997.

AC970853I